Inorg. Chem. **2009**, *48*, 3228−3238

Facile Synthesis of Bistridentate Ru^{II} Complexes Based on 2,6-Di(quinolin-8-yl)pyridyl Ligands: Sensitizers with Microsecond ^{3}MLCT Excited State Lifetimes

Michael Jäger,[†] Rohan J. Kumar,[†] Helmar Görls,[‡] Jonas Bergquist,[§] and Olof Johansson*,[†]

Department of Photochemistry and Molecular Science, Uppsala University, Box 523, 751 20 Uppsala, Sweden, Department of Inorganic and Analytical Chemistry, Friedrich-Schiller-Universität, 07743 Jena, Germany, Department of Physical and Analytical Chemistry, Uppsala University, Box 599, 751 24 Uppsala, Sweden

Received December 8, 2008

Synthetic routes to meridional bistridentate ruthenium(II) complexes based on 2,6-di(quinolin-8-yl)pyridyl (dqp) ligands have been investigated. Microwave-assisted synthesis at 200 °C allowed the high yield (49−87%) preparation of homoleptic meridional $[Ru(dqp)_2]^{2+}$-based complexes containing inert functional groups. Applying this protocol for the synthesis of *mer*-$[Ru(dqp)_2]^{2+}$ (*mer*-**1**) but lowering the temperature to 180 °C and shorter reaction times revealed the formation of the facial isomers *cis,fac*-**1** and *trans,fac*-**1** (56% and 12% yields, respectively). The facial isomers were characterized by NMR spectroscopy and X-ray diffraction analysis. In a stepwise protocol, the reaction of $Ru(dqp)Cl_3$ or $Ru(dqp)(L)Cl_2$ (L = MeCN or DMSO) and a second equivalent dqp gave *mer*-**1** in 12−26% yields and N_5Cl-coordinated $[Ru(dqp)_2Cl]^+$ (28−46%). $[Ru(dqp_2)Cl]^+$ was photochemically, or thermally in the presence of Ag^I, converted to *mer*-**1**. By using *mer*-$[Ru(dqp)(MeCN)_3]^{2+}$, which was crystallographically characterized, a wide range of homo- and heteroleptic meridional $[Ru(dqp)_2]^{2+}$-based complexes was synthesized in up to 77% yield. The synthetic utility of meridional $[Ru(dqp)_2]^{2+}$-based complexes as building blocks was demonstrated by palladium-catalyzed homocoupling of *mer*-$[Ru(dqp)(dqpPhBr)]^{2+}$ to form a dinuclear complex. The redox and photophysical properties of the meridional complexes are discussed.

Introduction

Ruthenium(II) polypyridyl complexes are frequently used as photosensitizers to study electron and energy transfer reactions. This is due to their often favorable photophysical properties which include long lifetimes of the excited metal-to-ligand charge transfer (^{3}MLCT) state.[1,2] In addition, geometrical considerations are important to control light-driven processes in donor-photosensitizer-acceptor (D-P-A) assemblies. However, the ideal *trans* geometry of the D and A units is not easily obtained using the prototypical $[Ru(bpy)_3]^{2+}$ (bpy is 2,2′-bipyridine) (Figure 1a). In contrast, $[Ru(tpy)_2]^{2+}$ (tpy is 2,2′:6′,2″-terpyridine) overcomes these structural limitations (Figure 1b),[3−5] but it is a less favorable photosensitizer because of very short ^{3}MLCT excited-state lifetime (τ = 0.25 ns for $[Ru(tpy)_2]^{2+}$).[6] The poor bite angle of the tpy ligand reduces the ligand field strength, leading to efficient thermal population of non-emissive metal-centered (MC) states.[7,8]

Strategies to increase the excited-state lifetimes of $[Ru(tpy)_2]^{2+}$-based complexes include functionalization in the

* To whom correspondence should be addressed. E-mail: olof.johansson@fotomol.uu.se.
† Department of Photochemistry and Molecular Science, Uppsala University.
‡ Friedrich-Schiller-Universität.
§ Department of Physical and Analytical Chemistry, Uppsala University.

(1) Meyer, T. J. *Pure Appl. Chem.* **1986**, *58*, 1193–1206.
(2) Juris, A.; Balzani, V.; Barigelletti, F.; Campagna, S.; Belser, P.; von Zelewsky, A. *Coord. Chem. Rev.* **1988**, *84*, 85–277.
(3) Sauvage, J.-P.; Collin, J.-P.; Chambron, J.-C.; Guillerez, S.; Coudret, C.; Balzani, V.; Barigelletti, F.; De Cola, L.; Flamigni, L. *Chem. Rev.* **1994**, *94*, 993–1019.
(4) Collin, J.-P.; Gavina, P.; Heitz, V.; Sauvage, J.-P. *Eur. J. Inorg. Chem.* **1998**, 1–14.
(5) Baranoff, E.; Collin, J.-P.; Flamigni, L.; Sauvage, J.-P. *Chem. Soc. Rev.* **2004**, *33*, 147–155.
(6) Winkler, J. R.; Netzel, T.; Creutz, C.; Sutin, N. *J. Am. Chem. Soc.* **1987**, *109*, 2381–2392.
(7) Medlycott, E. A.; Hanan, G. S. *Chem. Soc. Rev.* **2005**, *34*, 133–142.
(8) Medlycott, E. A.; Hanan, G. S. *Coord. Chem. Rev.* **2006**, *250*, 1763–1782.

10.1021/ic802342t CCC: $40.75
Published on Web 03/02/2009

4′-position of tpy,[9−11] extending the ligand π-system,[12−17] and the use of strong σ-donating ligands.[18−21] An alternative strategy is based on the incorporation of 6-membered chelates to enlarge the bite angle of the tridentate ligand and therefore increase the energy of the non-emissive MC states.[22−24] This approach led to the design of 2,6-di(quinolin-8-yl)pyridine (dqp), which shows meridional coordination of the two dqp ligands for $[Ru(dqp)_2]^{2+}$ (*mer*-**1**) in close to perfect octahedral geometry (Figure 1c).[25,26] The complex has an impressive 3 μs excited-state lifetime at room temperature and an emission quantum yield (ϕ) of 0.02. It was also demonstrated that *mer*-**1** is remarkably photostable and displays a high reactivity in light-induced electron and energy transfer processes with typical organic quenchers.[26]

Synthetic strategies to form bistridentate Ru^{II} complexes often rely on protocols developed for $[Ru(tpy)_2]^{2+}$-based complexes. Homoleptic complexes have been conveniently prepared from $RuCl_3 \cdot xH_2O$ under reducing conditions or from $Ru(DMSO)_4Cl_2$ with 2 equiv of tpy in refluxing EtOH.[27] The synthesis of heteroleptic complexes has been demonstrated in a two-step procedure via a Ru^{III} intermediate, $Ru(tpy)Cl_3$, prepared from $RuCl_3 \cdot xH_2O$ and 1 equiv of tpy in refluxing EtOH.[28] The insoluble material is used directly, or treated with Ag^{I} to afford an activated $[Ru(tpy)(solvate)_3]^{n+}$ intermediate, to form bisterpyridine complexes under reducing conditions.[29,30] Alternatively, $Ru(DMSO)_4Cl_2$ has recently been used as a Ru^{II} precursor in the synthesis of heteroleptic complexes via $Ru(tpy)(DMSO)Cl_2$.[31]

We previously reported the synthesis of *mer*-**1** (87% yield) using a microwave-assisted protocol at 200 °C.[25] The bis-amino substituted *mer*-$[Ru(dqpNH_2)_2]^{2+}$ was obtained in significantly lower yield (22%) because of the harsh reaction conditions.[26] The use of a milder stepwise protocol via a Ru^{III} intermediate also resulted in low yields of ethyl ester-substituted *mer*-$[Ru(dqpCO_2Et)_2]^{2+}$ and *mer*-$[Ru(dqp)(dqpCO_2Et)_2]^{2+}$ (both in 20% yields).[26] At that stage it was unclear what byproducts were formed and what the synthetic limitations were. To construct more sophisticated architectures (i.e., D-P-A complexes), the desired dqp-based Ru^{II} complexes must be readily accessible. With this motivation, a detailed study of the products of complexation reactions from a variety of precursors was undertaken and is presented here. In addition, the electrochemical and photophysical properties of a range of substituted complexes are examined and show that the favorable properties are maintained.

Experimental Section

Physical Measurements. NMR spectra were recorded on a JEOL 400 MHz spectrometer at 293 K. Chemical shifts are given in ppm and referenced internally to the residual solvent signal. Microwave heating was performed in an Initiator™ single mode microwave cavity at 2450 MHz (Biotage). High-resolution ESI-MS were performed on a superconducting 9.4 T FTICR mass spectrometer equipped with an in-house developed emitter.[32] HPLC-MS data were obtained on a Dionex Ultimate 3000 system on a Phenomenex Gemini C18 column (150 × 3.0 mm, 5 μ) coupled to Thermo LCQ Deca XP with electrospray ionization (ESI). Solvents used for HPLC: 0.05% HCO_2H in H_2O and 0.05% HCO_2H in MeCN. Preparative HPLC was performed on a C18 column (150 × 21.2 mm, 10 μ) with 0.1% HCO_2H in H_2O and 0.1% HCO_2H in MeCN as the eluents. Electrochemical experiments were performed with a three-electrode setup in a three-compartment cell connected to an Autolab potentiostat with a GPES electrochemical interface (Eco Chemie). The working electrode was a glassy carbon disk (diameter 3 mm, freshly polished). Potentials were measured versus a non-aqueous Ag/Ag^+ reference electrode (CH Instruments, 10 mM $AgNO_3$ in MeCN) with a potential of −0.080 V versus the ferrocenium/ferrocene ($Fc^{+/0}$) couple in MeCN. UV−vis absorption spectra were measured on a Varian Cary 50 instrument. Steady state emission measurements were performed on a Fluorolog 3-222 emission spectrometer from Jobin-Yvon and corrected for different detector sensitivity at different wavelengths. Time-resolved emission measurements were made with a frequency tripled Q-switched Nd:

(9) Maestri, M.; Armaroli, N.; Balzani, V.; Constable, E. C.; Cargill Thompson, A. M. W. *Inorg. Chem.* **1995**, *34*, 2759–2767.
(10) Constable, E. C.; Cargill Thompson, A. M. W.; Armaroli, N.; Balzani, V.; Maestri, M. *Polyhedron* **1992**, *11*, 2707–2709.
(11) Wang, J.; Fang, Y. Q.; Hanan, G. S.; Loiseau, F.; Campagna, S. *Inorg. Chem.* **2005**, *44*, 5–7.
(12) Fang, Y.-Q.; Taylor, N. J.; Laverdière, F.; Hanan, G. S.; Loiseau, F.; Nastasi, F.; Campagna, S.; Nierengarten, H.; Leize-Wagner, E.; Van Dorsselaer, A. *Inorg. Chem.* **2007**, *46*, 2854–2863.
(13) Polson, M. I. J.; Loiseau, F.; Campagna, S.; Hanan, G. S. *Chem. Commun.* **2006**, *1301*, 1303.
(14) Fang, Y.-Q.; Taylor, N. J.; Hanan, G. S.; Loiseau, F.; Passalacqua, R.; Campagna, S.; Nierengarten, H.; Van Dorsselaer, A. *J. Am. Chem. Soc.* **2002**, *124*, 7912–7913.
(15) Encinas, S.; Flamigni, L.; Barigelletti, F.; Constable, E. C.; Housecroft, C. E.; Schofield, E. R.; Figgemeier, E.; Fenske, D.; Neuburger, M.; Vos, J. G.; Zehnder, M. *Chem.—Eur. J.* **2002**, *8*, 137–150.
(16) Hissler, M.; El-ghayoury, A.; Harriman, A.; Ziessel, R. *Angew. Chem., Int. Ed.* **1998**, *37*, 1717–1720.
(17) Hammarström, L.; Barigelletti, F.; Flamigni, L.; Indelli, M. T.; Armaroli, N.; Calogero, G.; Guardigli, M.; Sour, A.; Collin, J.-P.; Sauvage, J.-P. *J. Phys. Chem. A* **1997**, *101*, 9061–9069.
(18) Son, S. U.; Park, K. H.; Lee, Y.-S.; Kim, B. Y.; Choi, C. H.; Lah, M. S.; Jang, Y. H.; Jang, D.-J.; Chung, Y. K. *Inorg. Chem.* **2004**, *43*, 6896–6898.
(19) Duati, M.; Tasca, S.; Lynch, F. C.; Bohlen, H.; Vos, J. G.; Stagni, S.; Ward, M. D. *Inorg. Chem.* **2003**, *42*, 8377–8384.
(20) Duati, M.; Fanni, S.; Vos, J. G. *Inorg. Chem. Commun.* **2000**, *3*, 68–70.
(21) Indelli, M. T.; Bignozzi, C. A.; Scandola, F.; Collin, J.-P. *Inorg. Chem.* **1998**, *37*, 6084–6089.
(22) Wolpher, H.; Johansson, O.; Abrahamsson, M.; Kritikos, M.; Sun, L.; Åkermark, B. *Inorg. Chem. Commun.* **2004**, *7*, 337–340.
(23) Abrahamsson, M.; Wolpher, H.; Johansson, O.; Larsson, J.; Kritikos, M.; Eriksson, L.; Norrby, P.-O.; Bergquist, J.; Sun, L.; Åkermark, B.; Hammarström, L. *Inorg. Chem.* **2005**, *44*, 3215–3225.
(24) Abrahamsson, M.; Lundqvist, M. J.; Wolpher, H.; Johansson, O.; Eriksson, L.; Bergquist, J.; Rasmussen, T.; Becker, H.-C.; Hammarström, L.; Norrby, P. O.; Åkermark, B.; Persson, P. *Inorg. Chem.* **2008**, *47*, 3540–3548.
(25) Abrahamsson, M.; Jäger, M.; Österman, T.; Eriksson, L.; Persson, P.; Becker, H.-C.; Johansson, O.; Hammarström, L. *J. Am. Chem. Soc.* **2006**, *128*, 12616–12617.
(26) Abrahamsson, M.; Jäger, M.; Kumar, R. J.; Österman, T.; Persson, P.; Becker, H.-C.; Johansson, O.; Hammarström, L. *J. Am. Chem. Soc.* **2008**, *130*, 15533–15542.
(27) See for instance: Schubert, U. S.; Hofmeier, H.; Newkome, G. R. *Modern Terpyridine Chemistry*; Wiley-VCH: Weinheim, 2006; pp 37−68, and references cited therein.
(28) Sullivan, B. P.; Calvert, J. M.; Meyer, T. J. *Inorg. Chem.* **1980**, *19*, 1404–1407.
(29) Constable, E. C.; Cargill Thompson, A. M. W.; Tocher, D. A.; Daniels, M. A. M. *New J. Chem.* **1992**, *16*, 855–867.
(30) Barigelletti, F.; Flamigni, L.; Balzani, V.; Collin, J.-P.; Sauvage, J.-P.; Sour, A.; Constable, E. C.; Cargill Thompson, A. M. W. *J. Am. Chem. Soc.* **1994**, *116*, 7692–7699.
(31) Ziessel, R.; Grosshenny, V.; Hissler, M.; Stroh, C. *Inorg. Chem.* **2004**, *43*, 4262–4271.
(32) Nilsson, S.; Wetterhall, J.; Bergquist, J.; Nyholm, L.; Markides, K. *Rapid Commun. Mass Spectrom.* **2001**, *15*, 1997–2000.

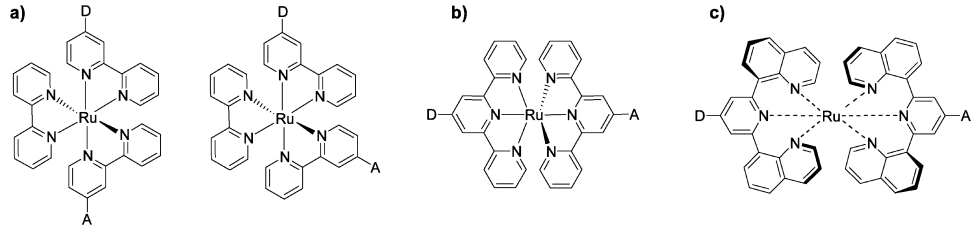

Figure 1. Donor−acceptor complexes based on (a) $[Ru(bpy)_3]^{2+}$ (2 of 4 geometrical isomers shown), (b) $[Ru(tpy)_2]^{2+}$, and c) $[Ru(dqp)_2]^{2+}$.

Table 1. Crystal Data and Refinement Details for the X-ray Structure Determinations

complex	*cis,fac*-**1**	*trans,fac*-**1**	*mer*-$[Ru(dqp)(MeCN)_3]^{2+}$
formula	$[C_{46}H_{30}N_6Ru]^{2+}$, $2(PF_6)^-$	$[C_{46}H_{30}N_6Ru]^{2+}$, $2(PF_6)^-$	$[C_{29}H_{24}N_6Ru]^{2+}$, $2(PF_6)^-$, 0.5 $C_4H_{10}O$, C_2H_3N
fw ($g\cdot mol^{-1}$)	1057.77	1057.77	925.67
T/°C	−90(2)	−90(2)	−90(2)
crystal system	triclinic	monoclinic	tetragonal
space group	$P\bar{1}$	$P2_1/c$	$P4_2/n$
a/ Å	12.9164(5)	7.7411(2)	25.5156(4)
b/ Å	13.0493(4)	22.3201(7)	25.5156(4)
c/ Å	14.2361(5)	11.5095(4)	12.5936(2)
α/deg	85.269(2)	90.00	90.00
β/deg	83.030(2)	94.901(2)	90.00
γ/deg	60.727(2)	90.00	90.00
V/Å^3	2076.87(13)	1981.36(11)	8199.0(2)
Z	2	2	8
ρ ($g\cdot cm^{-3}$)	1.691	1.773	1.500
μ (cm^{-1})	5.53	5.8	5.49
measured data	14771	12357	51384
data with $I > 2\sigma(I)$	8047	3587	6103
unique data/R_{int}	9364/0.0380	4503/0.0344	9387/0.0773
wR_2 (all data, on F^2)[a]	0.2393	0.0745	0.2687
R_1 ($I > 2\sigma(I)$)[a]	0.0795	0.0309	0.0823
S[b]	1.064	1.001	1.031
res. dens./e·Å^{-3}	1.480/-1.465	0.467/-0.477	2.272/-2.018
absorpt method	none	none	none
CCDC No.	711487	711488	711489

[a] Definition of the R indices: $R_1 = \sum||F_o| - |F_c||/\sum|F_o|$; $wR_2 = \{\sum[w(F_o^2 - F_c^2)^2]/\sum w(F_o^2)^2\}^{1/2}$ with $w^{-1} = \sigma^2(F_o^2) + (aP)^2$. [b] $s = \{\sum[w(F_o^2 - F_c^2)^2]/(N_o - N_p)\}^{1/2}$.

YAG laser (from Quantel) producing <10 ns flashes. Excitation light at 500 nm was obtained in an OPO. The emission was detected at right angle with a monochromator and a P928-type PMT. The PMT output was recorded on a Hewlett-Packard digital oscilloscope (2 Gsamples/s) and analyzed with a nonlinear least-squares algorithm with the Applied Photophysics LKS60 software. All emission measurements were performed in 1 × 1 cm quartz cuvettes in MeOH/EtOH (1:4). Illumination experiments were performed using a Schott KL 2500 LCD instrument as light source. The incident light was directed into a Pyrex glass bottle wrapped with aluminum foil through the lid using fiber optics.

X-ray Crystal Structure Analysis. Intensity data were collected on a Nonius Kappa CCD diffractometer using graphite-monochromated Mo Kα radiation. Data were corrected for Lorentz polarization but not for absorption effects.[33,34] The structures were solved by direct methods (SHELXS)[35] and refined by full-matrix least-squares techniques against F_o^2 (SHELXL-97).[36] The hydrogen atoms were included at calculated positions with fixed thermal parameters. Most of the non-hydrogen atoms were refined anisotropically.[36] DIAMOND was used for structure representations. (Table 1).

Materials. All commercially available reagents were used as received unless otherwise noted. $Ru(DMSO)_4Cl_2$,[37] $Ru(dqp)Cl_3$,[26] the dqpR ligands (R = -H, -CO_2Et, -PhMe, -PhBr, -Br, and -NH_2),[25,38] and 2,6-dibromo-4-hydroxypyridine[39] were prepared as described previously; 2,6-dibromo-4-methoxypyridine was prepared from 2,6-dibromo-4-hydroxypyridine adopting the literature protocol.[39] $Pd(dba)_2$ is bis(dibenzylideneacetone)palladium(0) and SPhos is 2-dicyclohexylphosphino-2′,6′-dimethoxybiphenyl. The Ru complexes were frequently treated with hexanes to make the complexes more crystalline. Residual hexanes therefore often appear in their elemental analysis.

4-Methoxy-2,6-di(quinolin-8-yl)pyridine (dqpOMe). Quinoline-8-boronic acid (0.283 g, 1.63 mmol), 2,6-dibromo-4-methoxypyridine (0.212 g, 0.79 mmol), $Pd(dba)_2$ (0.038 g, 0.065 mmol), SPhos (0.054 g, 0.133 mmol), and potassium carbonate (0.670 g, 4.85 mmol) were suspended in MeCN (10 mL) and H_2O (5 mL). The mixture was purged with argon and heated to 140 °C for 2 h in the microwave. After cooling to room temperature, H_2O was added and extracted (3×) with EtOAc. The combined organic layers were concentrated in vacuo and purified by column chromatography on silica using EtOAc/hexanes (10 to 99% EtOAc). Yield: 0.225 g, 78%. ^{1}H NMR ($CDCl_3$): δ 9.01 (dd, J = 4.2, 1.8 Hz, 2H), 8.24 (dd, J = 7.2, 1.5 Hz, 2H), 8.22 (dd, J = 8.3, 1.8 Hz, 2H), 7.87 (dd, J = 8.1, 1.5 Hz, 2H), 7.68 (s, 2H), 7.64 (dd, J = 8.1, 7.2 Hz, 2H),

(33) *COLLECT, Data Collection Software*; Nonius. B V. , Netherlands, 1998.
(34) Otwinowski, Z.; Minor, W. Processing of X-Ray Diffraction Data Collected in Oscillation Mode. In *Methods in Enzymology*; Carter, C. W., Sweet, R. M., Eds.; Academic Press: New York, 1997; Vol. *276*, Macromolecular Crystallography, Part A, pp 307−326.
(35) Sheldrick, G. M. *Acta Crystallogr.* **1990**, *A 46*, 467–473.
(36) Sheldrick, G. M. *SHELXL-97*, Release 97-2; University of Göttingen: Göttingen, Germany, 1997.
(37) Evans, I. P.; Spencer, A.; Wilkinson, G. *J. Chem. Soc., Dalton Trans.* **1973**, *204*, 209.
(38) Jäger, M.; Eriksson, L.; Bergquist, J.; Johansson, O. *J. Org. Chem.* **2007**, *72*, 10227–10230.
(39) Waki, M.; Abe, H.; Inouye, M. *Chem.—Eur. J.* **2006**, *12*, 7839–7847.

7.44 (dd, J = 8.3, 4.2 Hz, 2H), 3.98 (s, 3H), ^{13}C NMR: δ 164.9, 158.2, 150.3, 146.1, 139.6, 136.5, 131.6, 128.8, 128.7, 126.7, 121.0, 112.0, 55.4. MS (ESI): m/z 364 ([M + H]$^+$).

4-Hydroxy-2,6-di(quinolin-8-yl)pyridine (dqpOH). Quinoline-8-boronic acid (0.802 g, 4.63 mmol), 2,6-dibromo-4-hydroxypyridine (0.550 g, 2.17 mmol), $Pd(dba)_2$ (0.022 g, 0.038 mmol), SPhos (0.032 g, 0.078 mmol), and potassium carbonate (1.522 g, 11.01 mmol) were suspended in MeCN (10 mL) and H_2O (5 mL). The mixture was purged with argon and heated to 140 °C for 2 h in the microwave. After cooling to room temperature, silica was added and excess solvent removed in vacuo. The crude product was purified by column chromatography on silica using CH_2Cl_2/MeOH (1 to 10% MeOH). The combined fractions were washed with brine, and dried in vacuo. Yield: 0.527 g, 70%. ^{1}H NMR ($CDCl_3$): δ 8.63 (dd, J = 4.2, 1.8 Hz, 2H), 8.25 (dd, J = 8.3, 1.8, 2H), 8.19 (dd, J = 7.2, 1.3 Hz, 2H), 7.93 (dd, J = 8.2, 1.3 Hz, 2H), 7.64 (dd, J = 8.2, 7.4 Hz, 2H), 7.45 (dd, J = 8.3, 4.2 Hz, 2H), 7.09 (s, 2H), ^{13}C NMR: δ 180.3, 149.4, 147.7, 145.2, 137.2, 130.5, 130.1, 129.4, 128.8, 126.6, 121.5, 115.8. MS (ESI): m/z 350 ([M + H]$^+$), 698 ([2M + H]$^+$).

Microwave-Assisted Synthesis of Homoleptic Complexes. *mer*-[Ru(dqpPhMe)$_2$][PF$_6$]$_2$ (*mer*-2). A microwave vial was charged with dqpPhMe (0.041 g, 0.10 mmol), $Ru(DMSO)_4Cl_2$ (0.023 g, 0.05 mmol) and ethylene glycol (1.5 mL), sealed and heated to 200 °C for 5 min in the microwave. After cooling to room temperature, the solution was diluted with H_2O and aqueous NH_4PF_6 was added dropwise. The solids were filtered, washed with water and redissolved in MeCN. The crude product was purified by column chromatography on silica using MeCN/H_2O/sat. aq. KNO_3 (40:4:1) as the eluent. After counterion exchange with NH_4PF_6 and drying in vacuo, *mer*-**2** was obtained as a dark red powder. Yield: 0.037 g, 64%. ^{1}H NMR (CD_3CN): δ 8.15 (dd, J = 5.2, 1.5 Hz, 4H), 8.11 (s, 4H), 8.08 (dd, J = 8.3, 1.5 Hz, 4H), 7.90 (dd, J = 7.5, 1.4 Hz, 4H), 7.86 (m, 4H), 7.70 (dd, J = 8.3, 1.3 Hz, 4H), 7.48 (dd, J = 8.2, 7.4 Hz, 4H), 7.42 (m, 4H), 2.43 (s, 6H). HRMS (ESI) m/z 1093.1812 [M − PF$_6$]$^+$ (calcd for $C_{60}H_{42}F_6N_6PRu$ 1093.2156), 474.1279 [M − 2PF$_6$]$^{2+}$ (calcd for $C_{60}H_{42}N_6Ru$ 474.1257). Anal. Calcd for $C_{60}H_{42}F_{12}N_6P_2Ru\cdot H_2O\cdot 0.5C_6H_{14}$: C, 58.25; H, 3.96; N, 6.47; found: C, 58.22; H, 4.15; N, 6.43.

***mer*-[Ru(dqpOMe)$_2$][PF$_6$]$_2$(*mer*-3).** The complex was prepared as for *mer*-**2** using dqpOMe (0.027 g, 0.074 mmol) and $Ru(DMSO)_4Cl_2$ (0.017 g, 0.035 mmol) in ethylene glycol (1.5 mL). Purification by preparative HPLC using a gradient of MeCN/H_2O plus 0.1% HCO_2H (20 to 30% MeCN in 12 min) followed by counterion exchange with NH_4PF_6. Yield: 0.020 g, 49%. ^{1}H NMR (CD_3CN): δ 8.11 (dd, J = 5.2, 1.4 Hz, 4H), 8.04 (dd, J = 8.2, 1.4 Hz, 4H), 7.74 (dd, J = 7.5, 1.3 Hz, 4H), 7.66 (dd, J = 8.3, 1.4 Hz, 4H), 7.42 (dd, J = 8.2, 7.5 Hz, 4H), 7.05 (dd, J = 8.2, 5.2 Hz, 4H), 4.02 (s, 6H). HRMS (ESI) m/z 973.1070 [M − PF$_6$]$^+$ (calcd for $C_{48}H_{34}F_6N_6O_2PRu$ 973.1429), 414.0877 [M − 2PF$_6$]$^{2+}$ (calcd for $C_{48}H_{34}N_6O_2Ru$ 414.0894). Anal. Calcd for $C_{48}H_{34}F_{12}N_6O_2P_2Ru\cdot 2H_2O$: C, 49.96; H, 3.32; N, 7.28; found: C, 49.59; H, 3.44; N, 7.28.

***cis*,*fac*-[Ru(dqp)$_2$]$^{2+}$(*cis*,*fac*-1).** A microwave vial was charged with dqp (0.147 g, 0.441 mmol) and $Ru(DMSO)_4Cl_2$ (0.107 g, 0.221 mmol) and ethylene glycol (1.5 mL), sealed and heated to 180 °C for 5 min in the microwave. After cooling to room temperature, the solution was diluted with H_2O, and aqueous NH_4PF_6 was added dropwise. The solids were filtered, washed with water, and redissolved in MeCN. The crude product was purified by column chromatography on silica using MeCN/H_2O/sat. aq. KNO_3 (40:4:1) as eluent. The red band was collected, excess MeCN removed in vacuo, and the red solid filtered from the aqueous solution. The crude product was purified by preparative HPLC using a gradient of MeCN/H_2O plus 0.1% HCO_2H (12 to 17% MeCN in 70 min) followed by counterion exchange with NH_4PF_6. Yield: 0.118 g, 56%. ^{1}H NMR (CD_3CN): δ 8.69 (dd, J = 8.1, 1.4 Hz, 2H), 8.60 (dd, J = 5.3, 1.4 Hz, 2H), 8.27 (dd, J = 8.1, 1.3 Hz, 2H), 8.17 (dd, J = 8.1, 1.3 Hz, 2H), 8.14 (dd, J = 7.4, 1.3 Hz, 2H), 8.10 (dd, J = 8.1, 1.3 Hz, 2H), 7.83 (dd, J = 8.1, 5.3 Hz, 2H), 7.74 (t, J = 8.0 Hz, 2H), 7.70 (dd, J = 8.1, 7.4 Hz, 2H), 7.68 (dd, J = 5.3, 1.3 Hz, 2H), 7.63 (m, w = 15.6 Hz, 2H), 7.62 (dm, J = 8.0 Hz, 2H), 7.29 (dd, J = 7.5, 1.3 Hz, 2H), 7.14 (dd, J = 8.1, 1.3 Hz, 2H), 6.66 (dd, J = 8.1, 5.3 Hz, 2H). MS (ESI): m/z 384 ([M − 2PF$_6$]$^{2+}$). X-ray suitable crystals were obtained from vapor diffusion of Et_2O into a MeCN solution.

***trans*,*fac*-[Ru(dqp)$_2$]$^{2+}$(*trans*, *fac*-1).** The complex was isolated as a fraction from the synthesis of *cis*,*fac*-**1**. Yield: 0.025 g, 12%. ^{1}H NMR (CD_3CN): δ 9.18 (dd, J = 5.3, 1.4 Hz, 4H), 8.13 (dd, J = 8.2, 7.8 Hz, 2H), 8.05 (dd, J = 8.1, 1.4 Hz, 4H), 7.85 (dd, J = 7.5, 1.4 Hz, 4H), 7.80 (d, J = 8.1 Hz, 4H), 7.66 (dd, J = 8.1, 1.3 Hz, 4H), 7.48 (dd, J = 8.0, 7.5 Hz, 4H), 7.43 (dd, J = 8.1, 5.3 Hz, 4H). MS (ESI): m/z 384 ([M − 2PF$_6$]$^{2+}$). X-ray suitable crystals were obtained from vapor diffusion of Et_2O into a MeCN solution.

Synthesis of Ru(dqp)X$_3$ Precursors. Ru(dqp)(DMSO)Cl$_2$. To a solution of $Ru(dqp)Cl_3$ (0.100 g, 0.185 mmol) and DMSO (0.70 mL) in degassed chloroform (30 mL) was added triethylamine (2 mL). The resulting solution was stirred at reflux overnight under argon. The solution was cooled to room temperature washed with brine and dried over sodium sulfate. The solution was reduced in volume in vacuo before triturated with Et_2O. The solid was filtered from the solution, washed with Et_2O, and dried in vacuo to give a red solid. Yield: 0.055 g, 51%. ^{1}H NMR ($CDCl_3$): δ 9.75 (dd, J = 5.3, 1.1 Hz, 2H), 8.54 (d, J = 7.0 Hz, 2H), 8.43 (d, J = 7.4 Hz, 1H), 8.23 (d, J = 7.8 Hz, 2H), 7.99 (t, J = 9.7 Hz, 2H), 7.83 (t, J = 7.7 Hz, 2H), 7.56 (dd, J = 8.1, 5.4 Hz, 2H), 2.31 (s, 6H). Anal. Calcd for $C_{25}H_{21}Cl_2N_3ORuS$: C, 51.46; H, 3.63; N, 7.20; found: C, 51.27; H, 3.81; N, 7.19.

Ru(dqp)(MeCN)Cl$_2$. The complex was prepared as for Ru(dqp)-(DMSO)Cl_2 using MeCN instead of DMSO to give a dark purple solid. Yield: 0.061 g, 60%.^{1}H NMR (CD_3CN): δ 9.07 (dd, J = 5.1, 1.4 Hz, 2H), 8.61 (dd, J = 8.3, 1.4 Hz, 2H), 8.52 (dd, J = 7.5, 1.2 Hz, 2H), 8.26 (dd, J = 8.2, 1.2 Hz, 2H), 8.15 (dd, J = 8.4, 7.8 Hz, 1H), 7.98 (d, J = 8.1 Hz, 2H), 7.94−7.88 (m, 2H), 7.66 (dd, J = 8.2, 5.1 Hz, 2H), 2.43 (s, 3H). Anal. Calcd for $C_{25}H_{18}C1_2N_4Ru\cdot 0.5CH_3Cl\cdot 0.5EtOH$: C, 50.59; H, 3.44; N, 8.91; found: C, 50.20; H, 3.54; N, 8.56.

***mer*-[Ru(dqp)(MeCN)$_3$][PF$_6$]$_2$.** A suspension of $Ru(dqp)Cl_3$ (1.21 g, 2.22 mmol) and $AgNO_3$ (1.15 g, 6.76 mmol) in EtOH (5 mL), H_2O (5 mL) and MeCN (30 mL) was heated to 80 °C overnight. The mixture was allowed to cool to room temperature, filtered through a silica plug, and excess solvent was removed in vacuo. The crude product was purified by column chromatography on silica using MeCN/H_2O/sat. aq. KNO_3 (40:4:1) as the eluent. After counterion exchange with NH_4PF_6 and drying in vacuo, a bright yellow powder was obtained. Yield: 1.57 g, 84%. ^{1}H NMR (d_6-acetone): δ 9.39 (dd, J = 5.1, 1.5 Hz, 2H), 8.77 (dd, J = 8.2, 1.5 Hz, 2H), 8.74 (dd, J = 7.5, 1.3 Hz, 2H), 8.40 (dd, J = 8.2, 1.3 Hz, 2H), 8.31 (dd, J = 8.8, 7.2 Hz, 1H), 8.21 (m, 2H), 8.01 (dd, J = 8.2, 7.5 Hz, 2H), 7.77 (dd, J = 8.2, 5.1 Hz, 2H), 2.60 (s, 3H), 2.18 (s, 6H). MS (ESI): m/z 238 ([M − 2MeCN − 2PF$_6$]$^{2+}$), 279 ([M − 2PF$_6$]$^{2+}$). X-ray suitable crystals were obtained from vapor diffusion of Et_2O into a MeCN solution.

***mer*-[Ru(dqpCO$_2$Et)(MeCN)$_3$][PF$_6$]$_2$.** A microwave vial was charged with dqpCO_2Et (0.142 g, 0.35 mmol), $RuCl_3\cdot xH_2O$ (0.093 g, 0.36 mmol) and EtOH (15 mL), sealed and heated to 120 °C

overnight. The solids were filtered from the solution, washed with EtOH and Et_2O, and dried in vacuo. The crude Ru(dqpCO$_2$Et)Cl$_3$ and $AgNO_3$ (0.180 g, 1.06 mmol) were suspended in EtOH (5 mL), H_2O (5 mL), and MeCN (30 mL) and heated to 80 °C overnight. The mixture was allowed to cool to room temperature, filtered, and excess solvent was removed in vacuo.

The crude product was purified by column chromatography on silica using MeCN/H_2O/sat. aq. KNO_3 (40:4:1) as the eluent. After counterion exchange with NH_4PF_6 and drying in vacuo, a yellow powder was obtained. Yield: 0.262 g, 81% over 2 steps. ^{1}H NMR (d_6-acetone): δ 9.40 (dd, J = 5.1, 1.5 Hz, 2H), 8.83 (dd, J = 7.4, 1.2 Hz, 2H), 8.81 (dd, J = 8.3, 1.5 Hz, 2H), 8.49 (s, 2H), 8.46 (dd, J = 8.2, 1.2 Hz, 2H), 8.07 (dd, J = 8.2, 7.4 Hz, 2H), 7.79 (dd, J = 8.3, 5.1 Hz, 2H), 4.50 (q, J = 7.1 Hz, 2H), 2.62 (s, 3H), 2.20 (s, 6H), 1.41 (t, J = 7.1 Hz, 3H). MS (ESI): m/z 274 ([M − 2MeCN − 2PF$_6$]$^{2+}$), 315 ([M − 2PF$_6$]$^{2+}$).

***mer*-[Ru(dqpOH)(MeCN)$_3$][PF$_6$]$_2$.** The complex was prepared as for *mer*-[Ru(dqpCO$_2$Et)(MeCN)$_3$][PF$_6$]$_2$ using dqpOH (0.416 g, 1.19 mmol), $RuCl_3 \cdot xH_2O$ (0.320 g, 1.22 mmol) and EtOH (20 mL) to yield crude Ru(dqpOH)Cl$_3$ (0.540 g, 0.97 mmol). In the second step, Ru(dqpOH)Cl$_3$ (0.310 g, 0.556 mmol) and $AgNO_3$ (0.310 g, 1.823 mmol) were suspended in EtOH (10 mL), H_2O (2 mL), and MeCN (2 mL). Yield: 0.330 g, 55% over 2 steps. ^{1}H NMR (d_6-acetone): δ 9.38 (dd, J = 5.1, 1.5 Hz, 2H), 8.75 (dd, J = 8.2, 1.5 Hz, 2H), 8.69 (dd, J = 7.5, 1.3 Hz, 2H), 8.39 (dd, J = 8.2, 1.3 Hz, 2H), 7.99 (dd, J = 8.2, 7.5 Hz, 2H), 7.75 (dd, J = 8.2, 5.1 Hz, 2H), 7.64 (s, 2H), 2.58 (s, 3H), 2.18 (s, 6H). MS (ESI): m/z 246 ([M − 2MeCN − 2PF$_6$]$^{2+}$), 287 ([M − 2PF$_6$]$^{2+}$).

***mer*-[Ru(dqp)$_2$][PF$_6$]$_2$ (*mer*-1), Stepwise Synthesis via Ru(dqp)Cl$_3$.** To a suspension of Ru(dqp)Cl$_3$ (0.100 g, 0.185 mmol) and dqp (0.062 g, 0.185 mmol) in EtOH (5 mL) and H_2O (0.5 mL) was added *N*-ethylmorpholine (0.020 mL, 0.185 mmol). The mixture was heated at reflux overnight, allowed to cool to room temperature, poured into aqueous NH_4PF_6, and extracted with CH_2Cl_2. The crude product was purified by column chromatography on silica gel using MeCN/H_2O/sat. aq. KNO_3 (40:4:1) as the eluent. After counterion exchange with NH_4PF_6 and drying in vacuo, *mer*-**1** was obtained as a red powder. Yield: 0.023 g, 12%. The ^{1}H NMR data were identical to those reported previously.[25] [Ru(dqp)$_2$Cl][PF$_6$] was isolated as the major product. Yield: 0.080 g, 46%. ^{1}H NMR (CD_2Cl_2): δ 8.34 (dd, J = 4.2, 1.8 Hz, 1H), 8.26 (m, w = 17.4 Hz, 3H), 8.15 (m, w = 17.0 Hz, 3H), 8.05 (dd, J = 8.1, 1.5 Hz, 1H), 8.01 (d, J = 7.5 Hz, 2H), 7.94 (dd, J = 7.9, 1.5 Hz, 1H), 7.80 (dd, J = 8.8, 1.4 Hz, 1H), 7.74 (dd, J = 8.2, 1.6 Hz, 1H), 7.70 (dd, J = 6.9, 2.3 Hz, 1H), 7.64 (m, w = 17.0 Hz, 3H), 7.45 (m, w = 34.2 Hz, 3H), 7.32 (dd, J = 8.1, 5.3 Hz, 1H), 7.19 (dd, J = 8.3, 1.6 Hz, 1H), 7.15 (dd, J = 8.3, 4.2 Hz, 1H), 7.10 (dd, J = 5.2, 1.5 Hz, 1H), 7.04 (dd, J = 8.3, 1.4 Hz, 1H), 6.75 (dd, J = 7.4, 1.5 Hz, 1H), 6.70 (dd, J = 8.3, 7.0 Hz, 1H), 6.32 (dd, J = 8.1, 5.2 Hz, 1H), 6.20 (dd, J = 8.1, 5.3 Hz, 1H), 6.08 (dd, J = 7.00, 1.5 Hz, 1H). MS (ESI): m/z 803 ([M − PF$_6$]$^+$).

***mer*-[Ru(dqp)$_2$][PF$_6$]$_2$ (*mer*-1), Stepwise Synthesis via [Ru(dqp)(L)Cl$_2$] (L = MeCN).** A suspension of dqp (0.006 g, 0.018 mmol) and Ru(dqp)(MeCN)Cl$_2$ (0.010 g, 0.018 mmol) were stirred in EtOH/H_2O (9:1, 5 mL) at 80 °C overnight. The solution was poured into aqueous NH_4PF_6, extracted with CH_2Cl_2, and concentrated in vacuo. The crude product was purified by column chromatography using MeCN/H_2O/sat. aq. KNO_3 (40:4:1) as the eluent. After counterion exchange with NH_4PF_6, *mer*-**1** and [Ru(dqp)$_2$Cl][PF$_6$] were obtained in 26% and 46% yields, respectively.

***mer*-[Ru(dqp)$_2$][PF$_6$]$_2$ (*mer*-1), Stepwise Synthesis via [Ru(dqp)(L)Cl$_2$] (L = DMSO).** The complex was prepared as described above using dqp (0.006 g, 0.019 mmol) and Ru(dqp)(DMSO)Cl$_2$ (0.011 g, 0.019 mmol). Yields: 18% (*mer*-**1**) and 28% ([Ru(dqp)$_2$Cl][PF$_6$]).

Stepwise Synthesis via *mer*-[Ru(dqp)(MeCN)$_3$][PF$_6$]$_2$. *mer*-[Ru(dqp)$_2$][PF$_6$]$_2$ (*mer*-1). A flask was charged with *mer*-[Ru(dqp)(MeCN)$_3$][PF$_6$]$_2$ (0.124 g, 0.146 mmol), dqp (0.047 g, 0.141 mmol) and *n*-BuOH (5 mL). The mixture was heated to reflux overnight under a gentle argon flow. The mixture was cooled to room temperature, excess solvent was removed in vacuo. The crude product purified by column chromatography on silica using MeCN/H_2O/sat. aq. KNO_3 (40:4:1) as the eluent. The counterion was exchanged with NH_4PF_6 and dried in vacuo to give *mer*-**1** as a red powder. Yield: 0.108 g, 72%.

***mer*-[Ru(dqp)(dqpCO$_2$Et)][PF$_6$]$_2$ (*mer*-4).** The complex was prepared as for *mer*-**1** using *mer*-[Ru(dqp)(MeCN)$_3$][PF$_6$]$_2$ (0.131 g, 0.154 mmol), dqpCO$_2$Et (0.059 g, 0.146 mmol) and *n*-BuOH (5 mL). Yield: 0.127 g, 77%. The ^{1}H NMR data were identical to those reported previously.[26]

***mer*-[Ru(dqp)(dqpOMe)][PF$_6$]$_2$ (*mer*-5).** The complex was prepared as for *mer*-**1** using *mer*-[Ru(dqp)(MeCN)$_3$][PF$_6$]$_2$ (0.277 g, 0.33 mmol), dqpOMe (0.118 g, 0.33 mmol) and *n*-BuOH (4 mL). Yield: 0.211 g, 60%. ^{1}H NMR (CD_3CN): δ 8.13 (t, J = 8.1 Hz, 1H), 8.10 (dd, J = 5.2, 1.4 Hz, 2H), 8.06 (m, w = 13.7 Hz, 6H), 7.86 (d, J = 8.1 Hz, 2H), 7.77 (dd, J = 7.4, 1.3 Hz, 2H), 7.70 (dd, J = 7.5, 1.3 Hz, 2H), 7.67 (dd, J = 8.3, 1.3 Hz, 2H), 7.66 (dd, J = 8.4, 1.3 Hz, 2H), 7.44 (s, 2H), 7.43 (dd, w = 15.6 Hz, 4H), 7.06 (dd, J = 8.2, 5.2 Hz, 2H), 7.03 (dd, J = 8.0, 5.3 Hz, 2H), 4.03 (s, 3H). HRMS (ESI) m/z 943.0981 [M − PF$_6$]$^+$ (calcd for $C_{47}H_{32}F_6N_6OPRu$ 943.1323), 399.0844 [M − 2PF$_6$]$^{2+}$ (calcd for $C_{47}H_{32}N_6ORu$ 399.0841). Anal. Calcd for $C_{47}H_{32}F_{12}N_6OP_2Ru$: C, 51.89; H, 2.97; N, 7.73; found: C, 51.82; H, 3.26; N, 7.52.

***mer*-[Ru(dqp)(dqpPhBr)][PF$_6$]$_2$ (*mer*-6).** The complex was prepared as for *mer*-**1** using *mer*-[Ru(dqp)(MeCN)$_3$][PF$_6$]$_2$ (0.199 g, 0.235 mmol) and dqpPhBr (0.105 g, 0.215 mmol) in *n*-BuOH (10 mL). Yield: 0.160 g, 61%. ^{1}H NMR (CD_3CN): δ 8.17 (dd, J = 8.3, 7.8 Hz, 1H), 8.12 (dd, J = 5.2, 1.5 Hz, 2H), 8.08 (m, 8H), 7.88 (m, 6H), 7.77 (m, 2H), 7.73 (dd, J = 7.4, 1.4 Hz, 2H), 7.70 (m, 4H), 7.47 (m, 4H), 7.06 (m, 4H). HRMS (ESI) m/z 1069.0224 [M − PF$_6$]$^+$ (calcd for $C_{52}H_{33}F_6N_6{}^{81}BrPRu$ 1069.0615), 462.0385 [M − 2PF$_6$]$^{2+}$ (calcd for $C_{52}H_{33}N_6{}^{81}BrRu$ 462.0487). Anal. Calcd for $C_{52}H_{33}BrF_{12}N_6P_2Ru \cdot H_2O$: C, 50.74; H, 2.87; N, 6.83; found: C, 51.10; H, 3.17; N, 6.75.

***mer*-[Ru(dqp)(dqpBr)][PF$_6$]$_2$ (*mer*-7).** The complex was prepared as for *mer*-**1** using *mer*-[Ru(dqp)(MeCN)$_3$][PF$_6$]$_2$ (0.200 g, 0.236 mmol) and dqpBr (0.096 g, 0.233 mmol) in *n*-BuOH (5 mL). Yield: 0.190 g, 71%. ^{1}H NMR (CD_3CN): δ 8.17 (dd, J = 8.3, 7.8 Hz, 1H), 8.07 (m, 10H), 7.88 (d, J = 8.1 Hz, 2H), 7.70 (m, 8H), 7.46 (m, 4H), 7.08 (dd, J = 8.2, 5.3 Hz, 2H), 7.05 (dd, J = 8.2, 5.3 Hz, 2H). HRMS (ESI) m/z 992.9936 [M − PF$_6$]$^+$ (calcd for $C_{46}H_{29}F_6N_6{}^{81}BrPRu$ 993.0302), 424.0279 [M − 2PF$_6$]$^{2+}$ (calcd for $C_{46}H_{29}N_6{}^{81}BrRu$ 424.0330) Anal. Calcd for $C_{46}H_{29}BrF_{12}N_6P_2Ru \cdot 2H_2O \cdot 0.5C_6H_{14}$: C, 48.41; H, 3.32; N, 6.91; found: C, 48.43; H, 3.24; N, 7.14.

***mer*-[Ru(dqpCO$_2$Et)(dqpNH$_2$)][PF$_6$]$_2$ (*mer*-8).** The complex was prepared as for *mer*-**1** using *mer*-[Ru(dqpCO$_2$Et)(MeCN)$_3$][PF$_6$]$_2$ (0.100 g, 0.108 mmol) and dqpNH$_2$ (0.038 g, 0.108 mmol) in *n*-BuOH (1.5 mL). After column chromatography on silica, the impure product was purified by preparative HPLC using a gradient of MeCN/H_2O plus 0.1% HCO_2H (10 to 30% MeCN in 60 min). After counterion exchange with NH_4PF_6 and drying in vacuo, *mer*-**8** was obtained as a dark red powder. Yield: 0.012 g, 10%.^{1}H NMR (CD_3CN): δ 8.19 (s, 2H), 8.14 (dd, J = 5.1, 1.5 Hz, 2H), 8.05 (m, w = 16.4 Hz, 6H), 7.72 (dd, J = 7.4, 1.3 Hz, 2H), 7.66 (m, w = 21.7 Hz, 6H), 7.44 (dd, J = 8.2, 7.4 Hz, 2H), 7.42

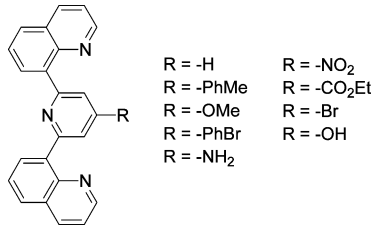

Figure 2. 4-Substituted 2,6-di(quinolin-8-yl)pyridyl ligands used in this study.

(dd, J = 8.2, 7,4 Hz, 2H), 7.11 (s, 2H), 7.09 (dd, J = 8.1, 5.2 Hz, 2H), 7.02 (dd, J = 8.1, 5.2 Hz, 2H), 5.61 (s br, 2H), 4.44 (q, J = 7.1, 2H), 1.40 (t, J = 7.1 Hz, 3H). HRMS (ESI) *m/z* 1000.1150 $[M - PF_6]^+$ (calcd for $C_{49}H_{35}F_6N_7O_2PRu$ 1000.1538), 427.5869 $[M - 2PF_6]^{2+}$ (calcd for $C_{49}H_{35}N_7O_2Ru$ 427.5948) Anal. Calcd for $C_{49}H_{35}F_{12}N_7O_2P_2Ru \cdot 1.5H_2O \cdot 0.5C_6H_{14}$: C, 51.41; H, 3.73; N, 8.07; found: C, 51.34; H, 3.76; N, 8.20.

***mer*-[Ru(dqpOH)(dqpBr)][PF$_6$]$_2$ (*mer*-9).** The complex was prepared as for *mer*-**1** using *mer*-[Ru(dqpOH)(MeCN)$_3$][PF$_6$]$_2$ (0.030 g, 0.035 mmol) and dqpBr (0.014 g, 0.034 mmol) in *n*-BuOH (1.5 mL). Yield: 0.013 g, 33%. ^{1}H NMR (CD_3CN): δ 8.11 (dd, J = 5.2, 1.5 Hz, 2H), 8.08 (dd, J = 5.2, 1.5 Hz, 2H), 8.04 (m, w = 17.2 Hz, 6H), 8.04 (s, 2H), 7.70 (dd, J = 7.5, 1.4 Hz, 2H), 7.67 (m, w = 8.6 Hz, 4H), 7.64 (dd, J = 8.1, 1.2 Hz, 2H), 7.41 (m, w = 23.5 Hz, 4H), 7.31 (s, 2H), 7.06 (dd, J = 8.2, 5.1 Hz, 4H). HRMS (ESI) *m/z* 1008.9876 $[M - PF_6]^+$ (calcd for $C_{46}H_{29}F_6N_6O^{81}BrPRu$ 1009.0251), 863.0218 $[M - H - 2PF_6]^+$ (calcd for $C_{46}H_{28}N_6O^{81}BrRu$ 863.0531), 432.0231 $[M - 2PF_6]^{2+}$ (calcd for $C_{46}H_{29}N_6O^{81}BrRu$ 432.0305). Anal. Calcd for $C_{46}H_{29}BrF_{12}N_6OP_2Ru \cdot 1.5C_6H_{14}$: C, 48.41; H, 3.32; N, 6.91; found: C, 48.43; H, 3.24; N, 7.14.

***mer*-[Ru(dqpCO$_2$Et)$_2$][PF$_6$]$_2$ (*mer*-10).** The complex was prepared as for *mer*-**1** using *mer*-[Ru(dqpCO$_2$Et)(MeCN)$_3$][PF$_6$]$_2$ (0.110 g, 0.120 mmol) and dqpCO$_2$Et (0.055 g, 0.135 mmol) in *n*-BuOH (10 mL). Yield: 0.060 g, 41%. The ^{1}H NMR data were identical to those reported previously.[26]

***mer*-[Ru(dqp)(dqpPhPhdqp)(dqp)Ru][PF$_6$]$_4$ (*mer*-11).** A microwave vial was charged with *mer*-**6** (0.081 g, 0.067 mmol), bis(neopentylglycolato)diboron (0.011 g, 0.042 mmol), potassium carbonate (0.028 g, 0.200 mmol), Pd(dba)$_2$ (0.002 g, 0.003 mmol), and SPhos (0.003 g, 0.008 mmol), sealed and backfilled with argon. After addition of DMF (dried from molecular sieves, 1 mL), the mixture was heated to 80 °C for 2 h. The crude product was purified by column chromatography on silica gel using MeCN/H_2O/sat. aq. KNO_3 (40:4:1, then 40:6:neat KNO_3) as the eluent. The slow-moving red band was collected, and the counterion exchanged with NH_4PF_6. Yield: 0.074 g, 78%. ^{1}H NMR (CD_3CN): δ 8.14 (m, w = 54.6 Hz, 26H), 7.95 (m, w = 37.4 Hz, 12H), 7.73 (m, w = 25.6 Hz, 12H), 7.49 (m, w = 26.9 Hz, 8H), 7.09 (m, w = 24.5 Hz, 8H). HRMS (ESI) *m/z* 988.1102 $[M - 2PF_6]^{2+}$ (calcd for $C_{104}H_{66}F_{12}N_{12}P_2Ru$ 988.1452), 610.4191 $[M - 3PF_6]^{3+}$ (calcd for $C_{104}H_{66}F_6N_{12}PRu$ 610.4421), 421.5768 $[M - 4PF_6]^{4+}$ (calcd for $C_{104}H_{66}N_{12}Ru$ 421.5905). Anal. Calcd for $C_{104}H_{66}F_{24}N_{12}P_4Ru_2 \cdot 2H_2O$: C, 54.27; H, 3.07; N, 7.30; found: C, 54.04; H, 3.28; N, 7.24.

Results and Discussion

The 2,6-di(quinolin-8-yl)pyridines shown in Figure 2 were used as ligands and were prepared as described previously.[25,38] They contain a range of functionalities that would be expected to modify the electronic properties of their respective Ru^{II} complexes and/or allow further functionalization.

Scheme 1. Synthesis of Meridional Homoleptic Complexes via Microwave Heating

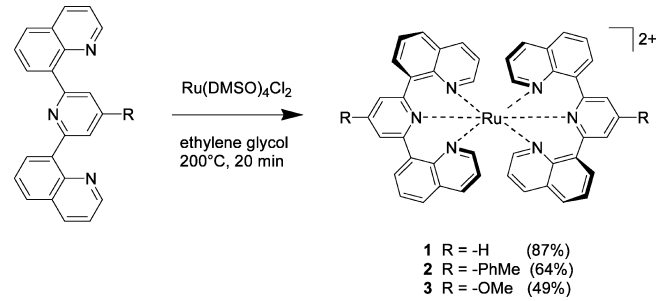

One-Step Microwave-Assisted Synthesis of Homoleptic Complexes. The *mer*-**2** and *mer*-**3** complexes were prepared from Ru(DMSO)$_4$Cl$_2$ using microwave heating in ethylene glycol at 200 °C for 20 min in good yields (49% and 64%, respectively) adopting the procedure reported for *mer*-**1** (Scheme 1).[25] Further attempts to form complexes containing more reactive functional groups, for example, R = -NH_2, -NO_2, -CO_2Et, or -Br, resulted in much lower yields or inseparable mixtures of complexes. Lowering the temperature did not result in improved yields, and it was generally observed that temperatures above 180 °C were required to form the bistridentate complexes in good yields. This is in contrast to $[Ru(tpy)_2]^{2+}$ which was synthesized in high yields at 120 °C within 5 min. Although the synthesis of *mer*-**1**−*mer*-**3** proved successful, the formation of complex mixtures prompted us to develop milder routes for the coordination reactions. These routes will be discussed in the paragraphs below.

Coordination Isomers of [Ru(dqp)$_2$]$^{2+}$. In the microwave-assisted synthesis of *mer*-**1**, small amounts of two additional Ru complexes, both displaying the identical mass and isotope pattern as *mer*-**1**, were detected by LC-MS. At 180 °C the two complexes form within 5 min in higher yields and were separated by column chromatography followed by preparative HPLC (56% and 12% yields, respectively).

The two complexes were shown to exhibit facial coordination by X-ray diffraction (Figure 3). This coordination mode is not observed for tpy based Ru complexes but is commonly observed for more flexible ligands such as *N*,*N*-bis(2-pyridylmethyl)ethylamine (bpea).[40] In the major byproduct (*cis*,*fac*-**1**), the two pyridines adopt a *cis*-configuration at the metal center, while the minor byproduct shows *trans*-coordination (*trans*,*fac*-**1**). The difference between *mer*-**1** and the facial isomers is the orientation of the two quinolines in each dqp ligand with respect to the central pyridine. In *mer*-**1**, the two quinolines point toward different faces of the pyridine resulting in a helical twist of the dqp ligand which allow the Ru^{II} ion to lie in plane with the N donors.[25,26] In the facial isomers, the two quinolines point toward the same face of the pyridine which causes a displacement of the Ru^{II} ion from the plane defined by the N donors (Figure 3). The

(40) Romero, I.; Rodríguez, M.; Llobet, A.; Collomb-Dunand-Sauthier, M.-N.; Deronzier, A.; Parella, T.; Stoeckli-Evans, H. *J. Chem. Soc., Dalton Trans.* **2000**, *1689*, 1694.

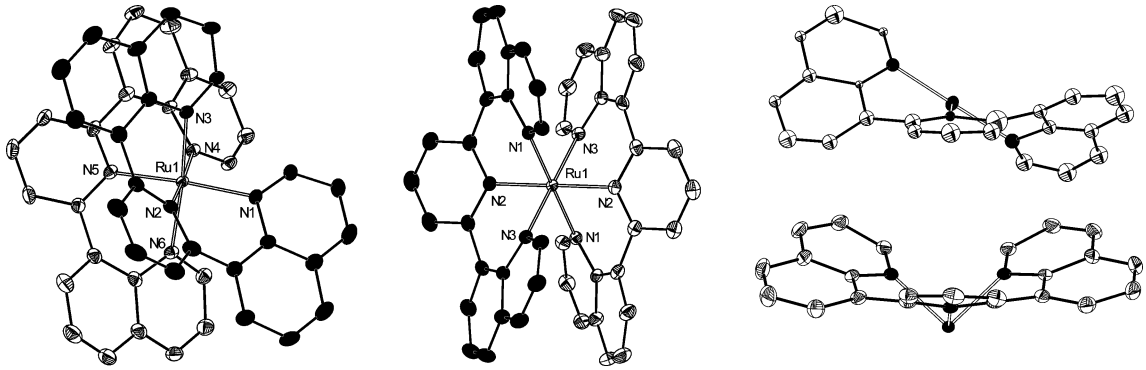

Figure 3. ORTEP views (40% probability ellipsoids) of *cis*,*fac*-**1** (left) and *trans*,*fac*-**1** (middle). Ligand orientation in *mer*-**1** (top right)[25,26] and *trans*,*fac*-**1** (bottom right). One dqp ligand omitted for clarity.

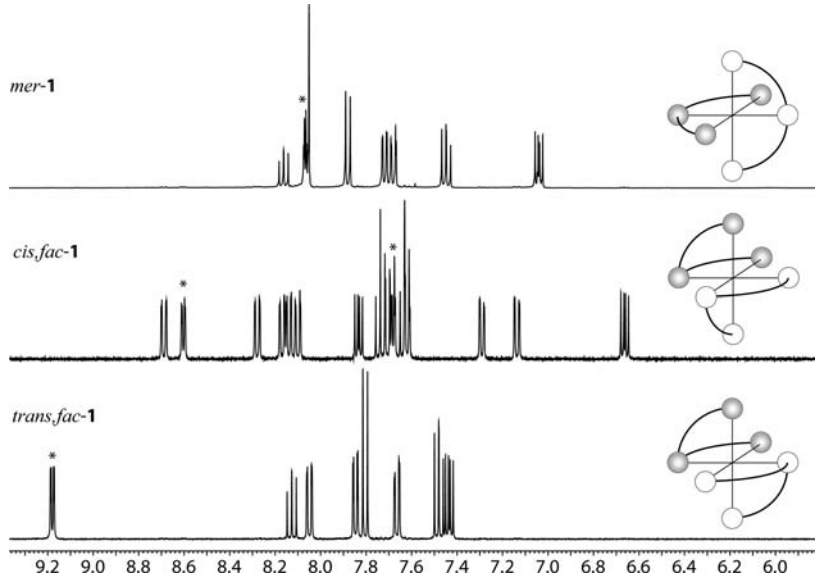

Figure 4. ^{1}H NMR spectra (400 MHz) of *mer*-**1**, *cis*,*fac*-**1**, and *trans*,*fac*-**1** in CD_3CN (as PF_6^- salts). The H^2 protons of the quinoline units are marked with an asterisk.

dihedral angles between the pyridine and the quinolines in the facial isomers are 23−28°, approximately 10° smaller compared to *mer*-**1**. The observed Ru−N (quinoline) bond distances are longer (2.092(3)−2.117(2) Å) than for Ru−N (pyridine) (2.037(3)−2.043(3) Å). All Ru−N bond distances in the facial isomers are somewhat elongated compared to *mer*-**1**.[25,26]

The *mer*-**1** complex is chiral and best described by the symmetry label D_2.[41] The dqp ligands are equivalent through a C_2 axis, and the ^{1}H NMR, which has been discussed in detail elsewhere,[38] shows one set of quinoline protons (Figure 4). In contrast to *mer*-**1**, the ^{1}H NMR spectrum of *cis*,*fac*-**1** shows two distinct quinoline units, and the complex is best described by the symmetry label C_2 and is therefore chiral. In agreement with the X-ray structure of *cis*,*fac*-**1**, the quinoline units within each ligand are different while the two dqp ligands are equivalent through a C_2 axis. A NOE interaction between the non-equivalent quinoline H^2 protons within the ligand further supports the *cis*-facial coordination mode. The *trans*,*fac*-**1** complex shows only one set of quinoline protons because of the higher symmetry (C_{2h}). The most notable feature of *trans*,*fac*-**1** is a downfield shift of the quinoline H^2 protons upon coordination (H^2 = 8.95 ppm in free ligand)[38] which is opposite to that observed for *mer*-**1** (Figure 4).

Extended heating of both *cis*,*fac*-**1** and *trans*,*fac*-**1** in ethylene glycol at 220 °C using microwave heating quantitatively generated the thermodynamically favored *mer*-**1**. The conversion to the meridional isomer has to invoke partial ligand de-coordination, and the possibility of ligand scrambling was investigated by repeating the isomerization in the presence of dqpPhMe. However, no ligand scrambling products were detected by LC-MS. Furthermore, the possibility to photoisomerize the facial isomers to *mer*-**1** was investigated, but no isomerization was observed after white light illumination in MeCN.

Stepwise Synthesis of Ru^{II} dqp-Based Complexes. Strategies for the stepwise formation of *mer*-**1** under mild conditions were explored (Scheme 2, Routes A−C). A $Ru(dqp)Cl_3$ precursor was initially prepared by the reaction of $RuCl_3 \cdot xH_2O$ with 1 equiv of dqp in EtOH at reflux for 3 h. Consecutive washings of the precipitated solid with Et_2O and EtOH showed continuous leeching of free ligand and

(41) In a previous report (ref 26), the presence of a 2-fold rotation axis in *mer*-**1** through the pyridyl 4-positions was referred to as quasi-C_{2v} symmetry in analogy to $[Ru(tpy)_2]^{2+}$. However, the complex is best described by the symmetry label D_2.

Scheme 2. Stepwise Synthetic Routes to *mer*-**1**[a]

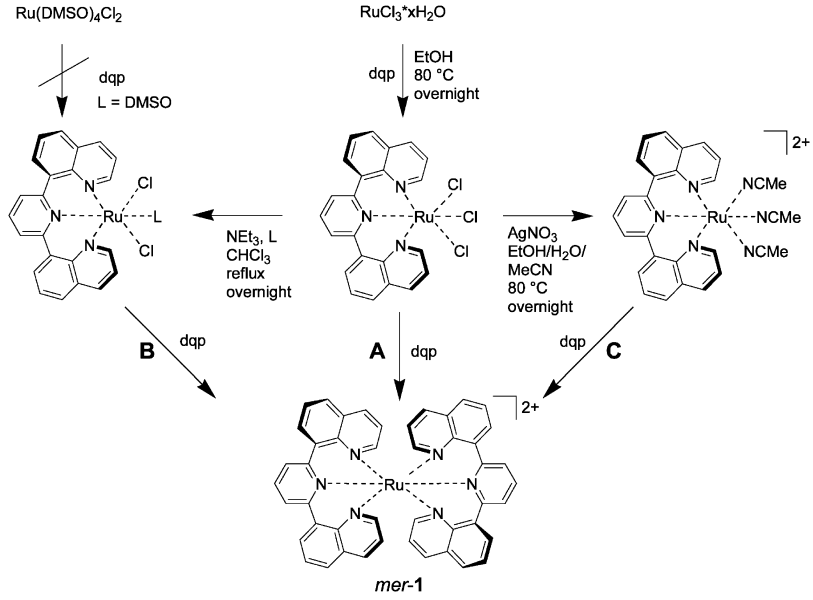

[a] Route (A) EtOH/H_2O, *N*-ethylmorpholine, 80 °C, overnight, (B) EtOH/H_2O, 80 °C, overnight, (C) *n*-BuOH, 120°C, overnight.

colored ruthenium-containing fractions, and it was observed that higher yields were obtained in subsequent steps if $Ru(dqp)Cl_3$ was prepared at 80−120 °C overnight. One should note the possibility for both facial and meridional coordination of the dqp ligand in the $Ru(dqp)Cl_3$ intermediate.

Via Ru(dqp)Cl$_3$ (Route A). The reaction of $Ru(dqp)Cl_3$ and dqp in the presence of *N*-ethylmorpholine as a reductant in a H_2O/EtOH mixture at reflux resulted in low yield of *mer*-**1** (12%) and significant amounts of a purple byproduct. This is in contrast to the higher yields reported for $[Ru(tpy)_2]^{2+}$ complexes using the analogous precursor under similar conditions.[27] On the basis of the observed high reaction temperatures required in the microwave-assisted protocol, the reaction was tested at 120 °C in *n*-BuOH at longer reaction times. However, the yield of *mer*-**1** did not increase significantly and instead *cis*,*fac*-**1** was detected in small amounts (<5%). The purple byproduct has the characteristic isotope pattern of a $[Ru(dqp)_2Cl]^+$ species and was assigned to a N_5Cl-coordinated species similar to $[Ru(tpyCl)_2Cl]^{+}$[42] (tpyCl is 4′-chloro-2,2′:6′,2″-terpyridine) and related complexes possessing N_5Cl coordination.[43]

The presence of one dangling quinoline unit in $[Ru(dqp)_2Cl]^+$ is supported by ^{1}H NMR which reveals an asymmetric complex with four different quinolines (Supporting Information). Analysis of the coupling constants of the quinoline subunits showed one distinct quinoline unit where the $^3J_{2,3}$ coupling constant is identical to free dqp ($^3J_{2,3}$ = 4.0 Hz). For all other quinolines in $[Ru(dqp)_2Cl]^+$, and also those in *mer*-**1**, *cis*,*fac*-**1** and *trans*,*fac*-**1**, the $^3J_{2,3}$ coupling constants are consistently larger compared to free dqp $\Delta^3J_{2,3}$ (+0.9 Hz).[44] From the ^{1}H NMR data, it was not possible to discern the detailed structure of $[Ru(dqp)_2Cl]^+$ regarding facial or meridional coordination (Supporting Information).

Scheme 3. Chemical and Photochemical Transformations of $[Ru(dqp)_2Cl]^+$

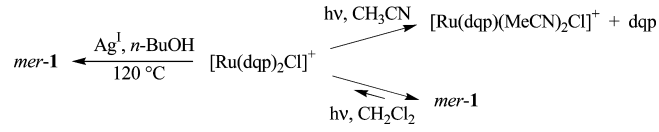

The potential for $[Ru(dqp)_2Cl]^+$ to form the desired *mer*-**1** complex was investigated. Treating $[Ru(dqp)_2Cl]^+$ with 1 equiv of $AgNO_3$ in EtOH at reflux overnight yielded $[Ru(dqp)_2NO_3]^+$ as supported by ESI-MS. In contrast, repeating the experiment in *n*-BuOH at 120 °C gave *mer*-**1**. When $[Ru(dqp)_2Cl]^+$ was irradiated with white light in MeCN, $[Ru(dqp)(MeCN)_2Cl]^+$, and free dqp were the main products while *mer*-**1** was predominently formed in weakly coordinating CH_2Cl_2. The observation that *mer*-**1** is formed from a $[Ru(dqp)_2Cl]^+$ intermediate in CH_2Cl_2 supports our previous finding that a photostationary state is reached when *mer*-**1** is irradiated in CH_2Cl_2 in the presence of excess chloride (Scheme 3).[26]

Via Ru(dqp)(L)Cl$_2$ (Route B). The use of $Ru(dqp)(L)Cl_2$ as synthetic intermediates avoids the in situ reduction of Ru^{III}, and potentially allow the introduction of redox-sensitive groups on the complex. Reacting $Ru(DMSO)_4Cl_2$ with 1 equiv of dqp in refluxing $CHCl_3$, as reported for tpy by Ziessel et al.[31] gave $[Ru(dqp)(DMSO)_4Cl]^+$ as identified by ESI-MS. The ^{1}H NMR spectrum reveals one set of quinoline protons with small chemical shift changes compared to free

(42) Constable, E. C.; Cargill Thompson, A. M. W. *Inorg. Chim. Acta* **1994**, *223*, 177–179.

(43) Jahng, Y.; Thummel, R. P.; Bott, S. G. *Inorg. Chem.* **1997**, *36*, 3133–3138.

(44) Only observed for H^3 in *mer*-**1** because of overlapping resonances for the H^2 proton, see ref 38. A similar change in the $^4J_{2,4}$ coupling constant upon coordination is also observed in all studied complexes ($\Delta^4J_{2,4}$ = −0.3 Hz).

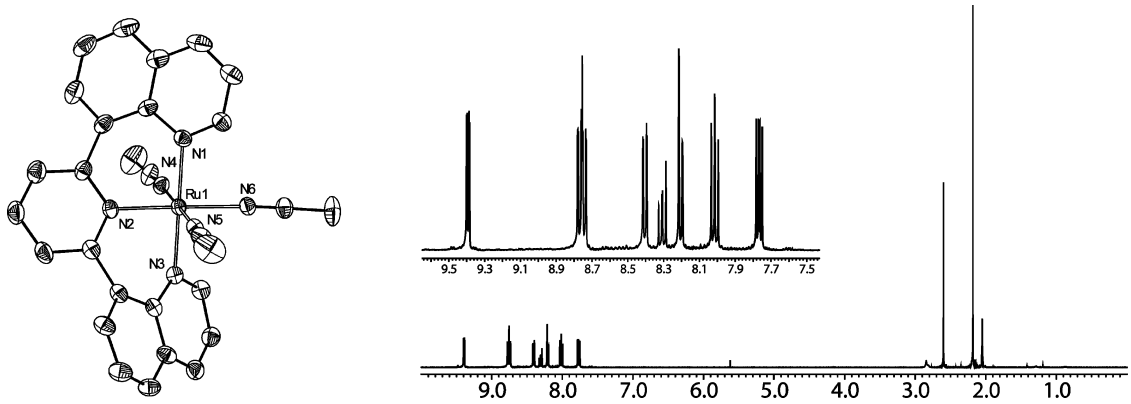

Figure 5. ORTEP view (40% probability ellipsoids) and ^{1}H NMR spectrum (400 MHz) of *mer*-[Ru(dqp)(MeCN)$_3$][PF$_6$]$_2$ (d$_6$-acetone).

dqp (Supporting Information), and the $^3J_{2,3}$ coupling constant is identical to the free ligand. This observation supports monodentate coordination of dqp via the central pyridine and is in line with the microwave-assisted synthesis where unusually high temperatures were required to form *mer*-**1** using Ru(DMSO)$_4$Cl$_2$.

The Ru(dqp)(L)Cl$_2$ intermediates (L = DMSO, MeCN) were instead successfully prepared via initial coordination of dqp to Ru^{III}. Ru(dqp)Cl$_3$ was treated with DMSO or MeCN in the presence of NEt$_3$ as a reductant to form Ru(dqp)(DMSO)Cl$_2$ or Ru(dqp)(MeCN)Cl$_2$, respectively, in good yields. The ^{1}H NMR spectra exhibit one set of quinoline protons, and ESI-MS and elemental analysis are in accordance to the assigned formulas. However, the coordination modes of dqp, either facial or meridional, remain unclear. The synthetic potential of these intermediates was subsequently assessed in an EtOH/H$_2$O mixture at reflux (see below, Table 2), but the yields of *mer*-**1** were not significantly improved compared to route A, and the N$_5$Cl- ([Ru(dqp)$_2$Cl]$^+$) and N$_6$-species were isolated in approximately a 2:1 ratio.

Via *mer*-[Ru(dqp)(MeCN)$_3$]$^{2+}$ (Route C). The preferential formation of undesired [Ru(dqp)$_2$Cl]$^+$ upon coordination of a second ligand to either Ru(dqp)Cl$_3$ or Ru(dqp)(L)Cl$_2$ motivated the preparation of a chloride-free mono-dqp Ru^{II} precursor where the initial coordination geometry could be determined. Heating Ru(dqp)Cl$_3$ in a EtOH/H$_2$O/MeCN mixture at 80 °C with 3 equiv of Ag^I gave *mer*-[Ru(dqp)(MeCN)$_3$]$^{2+}$ in 84% yield. The ^{1}H NMR spectrum shows the typical coupling pattern of tridentate-coordinated dqp with one set of quinoline protons (Figure 5). The two singlets at δ = 2.60 (3H) and 2.18 ppm (6H) were assigned to the MeCN ligands.

The meridional coordination was confirmed by X-ray crystal analysis (Figure 5). The Ru−N1 (2.073(5) Å) and Ru−N3 (2.068(5) Å) bond lengths to the quinoline nitrogens are slightly longer than the Ru−N2 (2.026(5) Å) bond to the central pyridine ring. All three Ru−N bond lengths to the MeCN ligands are within 2.018(5)−2.047(5) Å. The effect of the 6-membered chelates of the dqp ligand is manifested in the large bite angle, 179.9(2)°, which is close to the ideal angle for octahedral geometry. The dihedral angle between the pyridine ring and the quinoline units are 34.6(2)° and 40.2(2)°, respectively, and the dqp ligand adopts a similar helical twist as observed for *mer*-**1**.[25,26]

Reacting *mer*-[Ru(dqp)(MeCN)$_3$]$^{2+}$ with 1 equiv of dqp at reflux in EtOH showed little or very slow formation of *mer*-**1** or any other bistridentate products. However, *mer*-**1** was formed in high yield (72%) in *n*-BuOH at 120 °C with only little formation of *cis*,*fac*-**1** (<10%). Since pure *mer*-[Ru(dqp)(MeCN)$_3$]$^{2+}$ was used, some isomerization of the dqp ligand must have occurred under the experimental conditions.

From the present study, it is clear that the synthesis of meridional [Ru(dqp)$_2$]$^{2+}$-based complexes demand somewhat harsher conditions than for the related [Ru(tpy)$_2$]$^{2+}$. This is observed both in the formation of homoleptic complexes starting from Ru(DMSO)$_4$Cl$_2$ and in the second coordination of dqp to *mer*-[Ru(dqp)(MeCN)$_3$]$^{2+}$. A common feature of these reactions is the presence of coordinating solvents or anions (e.g., DMSO, MeCN, Cl$^-$) which prevent dqp coordination. The fact that tridentate coordination occurs more readily for [Ru(tpy)$_2$]$^{2+}$ suggests a larger steric barrier for formation of [Ru(dqp)$_2$]$^{2+}$. The success using *mer*-[Ru(dqp)(MeCN)$_3$]$^{2+}$ at 120 °C in *n*-BuOH is attributed to sufficient evaporation of MeCN and consequently depletion of the competing ligands since the reaction was found to be inhibited by excess MeCN.[45]

Stepwise Synthesis of Heteroleptic Complexes. The first heteroleptic dqp-based Ru^{II} complex *mer*-[Ru(dqp)(dqpCO$_2$Et)]$^{2+}$ (*mer*-**4**), prepared via route A, was previously reported.[26] Careful analysis of the reaction mixture revealed 20% yield of *mer*-**4**, 8% yield of *cis*,*fac*-**4**, and [Ru(dqp)(dqpCO$_2$Et)Cl]$^+$ (41%), in agreement with the results for *mer*-**1**. LC-MS analysis of the crude mixture also showed trace amounts of the homoleptic complexes *mer*-**1** and *mer*-**10** (Figure 6) which could be formed via ligand scrambling or from residual ligand or non-coordinated Ru species in Ru(dqp)Cl$_3$. To have a general route to heteroleptic complexes, it was important to study the potential for ligand scrambling using *mer*-[Ru(dqp)(MeCN)$_3$]$^{2+}$.

The *mer*-[Ru(dqp)(MeCN)$_3$]$^{2+}$ complex was reacted with dqpCO$_2$Et, dqpOMe, dqpPhBr, and dqpBr in *n*-BuOH at 120 °C overnight to form *mer*-**4** through *mer*-**7** in 60−77% yields (Figure 6 and Table 2). In all cases, the *cis*-facial isomers were formed as minor byproduct, while the ligand-scrambled products were only detected in trace amounts by LC-MS.

(45) The addition of Cl$^-$ also prevented tridentate dqp coordination and resulted in the formation of [Ru(dqp)$_2$Cl]$^+$].

Table 2. Isolated Yields of Meridional Complexes in the Stepwise Synthesis[a]

Ru-precursor	ligand	prod.	route	yield
$Ru(dqp)Cl_3$[b]	dqp	*mer*-**1**	A	12
$Ru(dqp)Cl_3$[b]	$dqpCO_2Et$	*mer*-**4**	A	20
$Ru(dqp)(MeCN)Cl_2$	dqp	*mer*-**1**	B	26
$Ru(dqp)(DMSO)Cl_2$	dqp	*mer*-**1**	B	18
mer-$[Ru(dqp)(MeCN)_3]^{2+}$	dqp	*mer*-**1**	C	72
mer-$[Ru(dqp)(MeCN)_3]^{2+}$	$dqpCO_2Et$	*mer*-**4**	C	77
mer-$[Ru(dqp)(MeCN)_3]^{2+}$	dqpOMe	*mer*-**5**	C	60
mer-$[Ru(dqp)(MeCN)_3]^{2+}$	dqpPhBr	*mer*-**6**	C	61
mer-$[Ru(dqp)(MeCN)_3]^{2+}$	dqpBr	*mer*-**7**	C	71
mer-$[Ru(dqpCO_2Et)(MeCN)_3]^{2+}$	$dqpNH_2$	*mer*-**8**	C	10
mer-$[Ru(dqpOH)(MeCN)_3]^{2+}$	dqpBr	*mer*-**9**	C	33
mer-$[Ru(dqpCO_2Et)(MeCN)_3]^{2+}$	$dqpCO_2Et$	*mer*-**10**	C	41

[a] As PF_6^- salts. [b] Ref 26. Conditions A: $EtOH/H_2O$, *N*-ethylmorpholine, 80 °C, overnight. B: $EtOH/H_2O$, 80 °C, overnight. C: *n*-BuOH, 120 °C overnight.

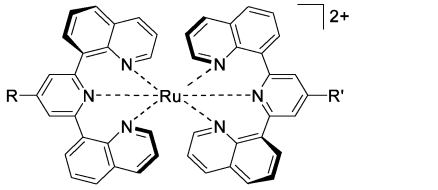

mer-**1** R, R' = -H
mer-**4** R = H, R' = $-CO_2Et$
mer-**5** R = H, R' = -OMe
mer-**6** R = H, R' = -PhBr
mer-**7** R = H, R' = -Br
mer-**8** R = $-CO_2Et$, R' = $-NH_2$
mer-**9** R = -OH, R' = -Br
mer-**10** R = $-CO_2Et$, R´= $-CO_2Et$

Figure 6. Meridional $[Ru(dqp)_2]^{2+}$-based complexes synthesized via *mer*-$[Ru(dqp\text{-}R)(MeCN)_3]^{2+}$.

The complexes were easily purified by column chromatography. To further expand the scope of the reaction, the hydroxyl- and amino-containing complexes *mer*-**8** and *mer*-**9** were prepared in modest yields using the readily accessible *mer*-$[Ru(dqpCO_2Et)(MeCN)_3]^{2+}$ and *mer*-$[Ru(dqpOH)(MeCN)_3]^{2+}$ as intermediates (Table 2). In the synthesis of *mer*-**8**, more extensive ligand scrambling was observed (Supporting Information) and purification of the complex required additional preparative HPLC. This behavior is attributed to decomposition of *mer*-$[Ru(dqpCO_2Et)(MeCN)_3]^{2+}$ during the reaction since no scrambling occurs from the formed bis-dqp complex (see above). Along these lines, the yield of homoleptic *mer*-**10** using the same precursor is somewhat lower than for *mer*-**4** through *mer*-**7** (Table 2). In general, *mer*-$[Ru(dqp)(MeCN)_3]^{2+}$ and its derivatives offer a viable route to homo- and heteroleptic complexes using relatively mild conditions.[46]

C−C Homocoupling of Bromo-Substituted *mer*-6. The use of substituted $[Ru(dqp)_2]^{2+}$-based complexes as building blocks for more sophisticated architectures was demonstrated by the synthesis of the dinuclear complex *mer*-**11** (Figure 7) via Pd-catalyzed homocoupling of *mer*-**6**. Similar metal-catalyzed cross-couplings and homo-couplings of transition metal polypyridyl complexes have been established as an important tool to synthesize di- and multinuclear species.[47−50] Initial attempts to form the complex by the reaction

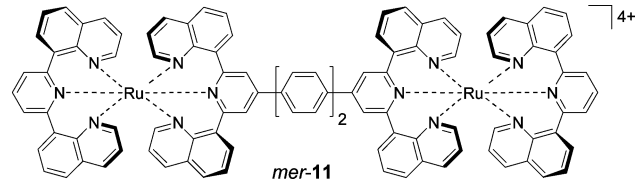

Figure 7. Dinuclear complex *mer*-**11**.

of dqp-Ph_2-dqp[38] and 2 equiv of *mer*-$[Ru(dqp)(MeCN)_3]^{2+}$ gave an inseparable mixture of complexes, presumably because of both facial and meridional coordination at the Ru^{II} centers.[51] However, the dimerization of *mer*-**6** (via in situ boronic ester formation and subsequent Suzuki coupling) proceeded efficiently to give *mer*-**11** in 78% yield following the same protocol as for the synthesis of dqp-Ph_2-dqp.[38]

Electrochemical and Photophysical Properties. The *mer*-**1** through *mer*-**11** complexes and *mer*-$[Ru(dqp)(MeCN)_3]^{2+}$ were studied by cyclic voltammetry (CV) in MeCN, and the electrochemical potentials are reported in Table 3 (vs $Fc^{+/0}$). Assignments of the redox processes were made analogously to previously studied dqp-based Ru^{II} complexes and are supported by the DFT calculations reported for *mer*-**1**.[26] The highest occupied molecular orbitals (HOMO) are essentially pure Ru 4d (t_{2g}) orbitals while the three lowest unoccupied orbitals are ligand centered π^* orbitals. All complexes show a reversible one-electron metal-based oxidation where the potential varies as expected with the electron-donating/electron-accepting properties of the substituents.[9,29,52,53] For the dinuclear *mer*-**11**, a single two-electron oxidation was observed indicating little metal−metal interaction.[54] A reversible ligand-based one-electron reduction occurs at $-1.76 \leq E_{1/2} \leq -1.52$ V for all complexes except *mer*-**7** and *mer*-**9** which show irreversible reduction, and differential pulse voltammetry (DPV) data are reported instead. The reductions also vary as expected from the substituent effects. For *mer*-**11**, the first one-electron reduction occurs as less negative potential than for *mer*-**1** or *mer*-**2** suggesting reduction of the bridging ligand. The *mer*-$[Ru(dqp)(MeCN)_3]^{2+}$ complex also shows reversible redox couples, with a one-electron metal-centered oxidation at +1.06 V and two reduction waves at −1.75 and −1.97 V, respectively.

The absorption spectra and room temperature emission data were collected for *mer*-**1** to *mer*-**11** and are presented in Table 3. All display strong ^{1}MLCT transitions in the visible region with extinction coefficients between 1.0 to 1.4 $\times 10^4$ M^{-1} cm^{-1}, except *mer*-**11** that exhibits a much stronger absorption because of the two metal centers. The *cis*,*fac*-**1** and *trans*,*fac*-**1** complexes show distinct absorption spectra with ^{1}MLCT bands that are more structured and red-shifted

(46) The complexes are stable and can be stored under nitrogen for weeks without noticeable decomposition.
(47) Johansson, K. O.; Lotoski, J. A.; Tong, C. C.; Hanan, G. S. *Chem. Commun.* **2000**, *819*, 820.
(48) Aspley, C J.; Gareth Williams, J. A. *New J. Chem.* **2001**, *25*, 1136–1147.
(49) Arm, J. A.; Gareth Williams, J. A. *Chem. Commun.* **2005**, *230*, 232.
(50) Arm, K. J.; Gareth Williams, J. A. *Dalton Trans.* **2006**, *2172*, 2174.
(51) Purification was further complicated because of the similar retention time of the Ru^{II} and $Ru_2^{II,\,II}$ species upon column chromatography on silica and preparative HPLC. Attempted isomerization above 200 °C resulted in decomposition of the complexes.
(52) Fallahpour, R.-A. *Eur. J. Inorg. Chem.* **1998**, *120*, 5–1207.
(53) Fallahpour, R.-A.; Neuburger, M.; Zehnder, M. *New J. Chem.* **1999**, *5*, 3–61.
(54) Ward, M. D. *Chem. Soc. Rev.* **1995**, *24*, 121–134.

Table 3. Electrochemical and Photophysical Properties

complex[a]	$E_{1/2}$/V[b] (ΔE_p/mV)			photophysical properties			
	$Ru^{III/II}$	$L^{0/-}$	$L^{-/2-}$	abs (M^{-1} cm^{-1})($\varepsilon \times 10^{-4}$)	Ems (nm)[c]	$\tau/\mu s$[c]	Φ[c]
mer-**1**[d]	0.71 (63)	−1.73 (62)	−1.90[e]	491(1.4)	700	3.0	0.02
mer-**2**	0.64 (63)	−1.73 (62)	−1.86[e]	552(1.1)	694[f]	2.3[f]	0.04[f]
mer-**3**	0.56 (66)	−1.76 (57)	−1.93 (49)	502(1.0)	718	1.2	0.005
mer-**4**[d]	0.77 (77)	−1.58 (74)	−1.89 (84)	492(1.0)	706	4.3	0.04
mer-**5**	0.63 (70)	−1.75 (60)	−1.92 (60)	498(1.2)	702	2.0	0.01
mer-**6**	0.69 (60)	−1.71 (56)	−1.87 (101)	496(1.4)	690	3.0	0.03
mer-**7**	0.73 (64)	−1.62[e]	−1.74[e]	492(1.2)	693	2.9	0.02
mer-**8**	0.57 (71)	−1.65 (59)	−1.97 (91)	521(1.1)	741	2.0	0.02
mer-**9**	0.65 (64)	−1.66[e]	−1.88[e]	510(1.0)	759	0.5	0.003
mer-**10**[d]	0.82 (69)	−1.52 (65)	−1.73 (66)	553(1.0)	693	5.5	0.07
mer-**11**	0.69 (72)	−1.68 (64)	−1.84[e]	500(3.1)	690	2.8	0.02
mer-$[Ru(dqp)(MeCN)_3]^{2+}$	1.06 (71)	−1.75 (65)	−1.97 (73)	n.d.	n.d.	n.d.	n.d.

[a] As PF_6^- salts. [b] $TBAPF_6$, MeCN, 0.1 V/s, vs $Fc^{+/0}$. [c] 298 K, deoxygenated MeOH/EtOH solutions. [d] Ref 26. [e] DPV peak potential. [f] 298 K, deoxygenated MeCN.

compared to *mer*-**1** (Supporting Information). The effect of coordination mode on the photophysical properties is currently under investigation and will be reported in due course. In analogy to previously reported $[Ru(dqp)_2]^{2+}$-based complexes, the meridional complexes have high emission yields (up to 0.07) with exceptionally long microsecond excited-state lifetimes. This confirms our previous findings that the favorable geometrical properties of $[Ru(dqp)_2]^{2+}$-based complexes can be combined with various substituents on the 4-position of the central pyridine and still obtain excellent photophysical properties with long excited-state lifetimes, even longer than those obtained in most trisbidentate Ru^{II} complexes.

Conclusions

Since the first report of *mer*-**1** and its potential use as a sensitizer for rod-like molecular arrays, substantial progress in the synthesis of this promising new type of complexes was made. While tpy shows only meridional coordination, dqp forms both meridional and facial bistridentate Ru^{II} complexes with the former as the thermodynamic product. In addition to this structural variation, it was found that dqp has a lower preference to form tridentate complexes of Ru^{II} than tpy. The presence of coordinating species precluded the direct application of protocols developed for tpy. This limitation was overcome with the chloride-free *mer*-$[Ru(dqp)(MeCN)_3]^{2+}$ precursor, which allowed the facile synthesis of a range of meridional bistridentate complexes. The use of $[Ru(dqp)_2]^{2+}$-based complexes as building blocks for novel architectures was exemplified by a palladium-catalyzed homo-coupling forming a dinuclear complex. All complexes maintain their excellent photophysical properties including microsecond excited-state lifetimes at room temperature. We are currently adopting this synthetic route in the synthesis of novel donor−acceptor assemblies for vectorial photoinduced charge separation.

Acknowledgment. We thank Professor Leif Hammarström, Professor Jean-Pierre Sauvage, and Dr. Lars Eriksson for stimulating discussions. This work was financially supported by the Swedish Energy Agency, the Knut and Alice Wallenberg foundation, and the EU/Energy Network project SOLAR-H2 (FP7 contract 212508).

Supporting Information Available: UV−vis absorption spectra of *mer*-**1**, *cis*,*fac*-**1**, and *trans*,*fac*-**1**, ^1H NMR spectra of $[Ru(dqp)_2Cl]^+$ and $[Ru(dqp)(DMSO)_4Cl]^+$, LC-UV chromatogram of crude $[Ru(dqpCO_2Et)(dqpNH_2)]^{2+}$. X-ray crystallographic data for *cis*,*fac*-**1**, *trans*,*fac*-**1**, and *mer*-$[Ru(dqp)(MeCN)_3]^{2+}$ in the form of CIF file data. This material is available free of charge via the Internet at http://pubs.acs.org.

IC802342T